International Journal of
Energy & Technology

ISSN 2035-911X

International Journal of Energy & Technology 5 (20) (2013) 1–10

STEADY NATURAL CONVECTION FLOW IN A VERTICAL RECTANGULAR DUCT WITH ISOTHERMAL WALL BOUNDARY CONDITIONS

J.C. Umavathi[1], Ali J. Chamkha[2]

[1]Department of Mathematics, Gulbarga University, Karnataka, India, E-mail: jc_uma11@yahoo.com
[2]Manufacturing Engineering Department, The Public Authority for Applied Education and Training, Shuweikh 70654, Kuwait, E-mail: achamkha@yahoo.com

ABSTRACT

Numerical investigation of steady natural convection flow in a vertical rectangular duct is investigated. One of the vertical walls of the duct is cooled to a constant temperature while the other wall is heated to constant but different temperatures. The other two sides of the duct are insulated. The nonlinear coupled partial differential equations governing the flow have been solved numerically using finite difference method. The problem is analyzed for different values of Grashof number, Brinkman number and aspect ratio. It is found that the Grashof number, Brinkman number and aspect ratio increase the velocity and temperature. The volumetric flow rate, the shear stress and the rate of heat transfer are presented as a function of Grashof number, Brinkman number and aspect ratio.

Keywords: Natural convection; viscous dissipation; finite difference method; rectangular duct.

1. INTRODUCTION

The phenomenon of natural convection in enclosures has received considerable attention in recent years. This attention is mainly due to because this phenomenon often affects the thermal performance in many engineering and science applications such as boilers, nuclear reactor systems, energy storage and conservation, fire control and chemical, food and metallurgical industries.

Buoyancy driven flows are complex because of essential coupling between the transport properties of flow and thermal fields. Among the earlier studies, it may be noted that Fusegi et al. [1], Lage and Bejan [2,3], and Xia and Murthy [4] have made attempt to acquire a basic understanding of natural convection flows and transfer characteristics in an enclosure where one of the vertical wall is cooled and another one heated while the remaining top and bottom walls are insulated. November and Nansteel [5] and Valencia and Frederick [6] have shown a specific interest to focus on a natural convection within a rectangular enclosure wherein a bottom heating and/or a top cooling are involved. Studies on natural convection in a rectangular enclosure heated from below and cooled along a single side or both sides have been carried out by Ganzarolli and Milanez [7]. Corcione [8] have studied a natural convection in an air-filled rectangular enclosure heated from below and cooled from above for a variety of thermal boundary conditions at the side walls. Numerical results were reported for several values of both width-to-height aspect ratio of enclosure and Rayleigh number. Interesting reviews of the theoretical studies on this subject have been presented in (Gebhart et al. [9], Bejan [10]).

The shape of a rectangular cavity is determined by the value of the aspect ratio *A*, given by the height to width ratio. Analytical solutions refer either to tall enclosures $(A >> 1)$ or to shallow enclosures $(A << 1)$. The mean Nusselt number for tall enclosures with vertical isothermal walls has been evaluated by Gill [11] and by Bejan [12]. The mean Nusselt number for shallow enclosures has been evaluated in (Cormack et al. [13], Bejan and Tien [14], Shiralkar and Tien [15]). As it has been pointed out by Bejan [12], when the parameter A has values close to 1, analytical or semi-analytical techniques are no longer applicable: in this case, numerical solutions and experimental investigations must be employed.

Many numerical or experimental papers on natural convection in vertical or inclined rectangular cavities are available in the literature (Ozoe et al. [16], De Vahl Davis [17], Hamadi et al. [18], Adjlout et al. [19]). An accurate benchmark solution for free convection of air $(\mathrm{Pr} = 0.71)$ in a square cavity with vertical boundaries kept at different temperatures is presented in De Vahl Davis [17] with reference to $10^3 < Ra < 10^6$. In Hamadi et al. [18] an experimental and numerical analysis of free convection of air in a square inclined cavity is presented. The authors provide an experimental correlation for the mean Nusselt number, in the range $10^4 < Ra < 10^6$, which is in good agreement with the numerical results reported in De Vahl Davis [17].

The viscous dissipation effect, which is a local production of thermal energy through the mechanism of viscous stresses, is a ubiquitous phenomenon and it is encountered in the viscous flow of clear fluid. There are some applications where one is willing to inspect the viscous dissipation effects. In an analysis of mantle flow, Bercovici [20] showed an example of the effects of viscous dissipation in self-lubricating systems. On the other hand, the recent work of Celata et al. [21] addresses an interesting

application of viscous dissipation in measuring the fluid friction coefficient for flow in a micro- channel. In another notable study, Murakami and Mikic [22] have stated that even for flow of air, which has a relatively small viscosity compared to common liquids, say water, through a micro-channel one should consider the effects of viscous dissipation when it comes to seek an optimum design feature for either of laminar or turbulent flows.

Regardless of its importance in engineering applications, free convection heat and mass transfer in vertical rectangular ducts has not been well evaluated. This motivates the present investigation. The purpose of this study is to examine the effects of buoyancy forces in vertical rectangular duct in the presence of viscous dissipation.

2. MATHEMATICAL FORMULATION

Figure 1 displays the schematic diagram of the two-dimensional rectangular vertical duct in this study. The length and breadth of the rectangular cross-section of the duct are a and b. It is assumed that the two sides of the duct are maintained at constant different temperatures T_1 at $Y=0$ and T_2 at $Y=b$, where $T_2 > T_1$. The other two sides of the duct are insulated, i.e. they are maintained at $\frac{\partial T}{\partial X}=0$ at $X=a$ and $X=0$. Fluid rises in the duct driven by buoyancy forces. The Oberbeck-Boussinesq approximation is supposed to hold $\left(\rho=\rho_0\left(1-\beta\left(T-T_0\right)\right)\right)$. Hence the flow is due to difference in temperature and the convection sets in instantaneously.

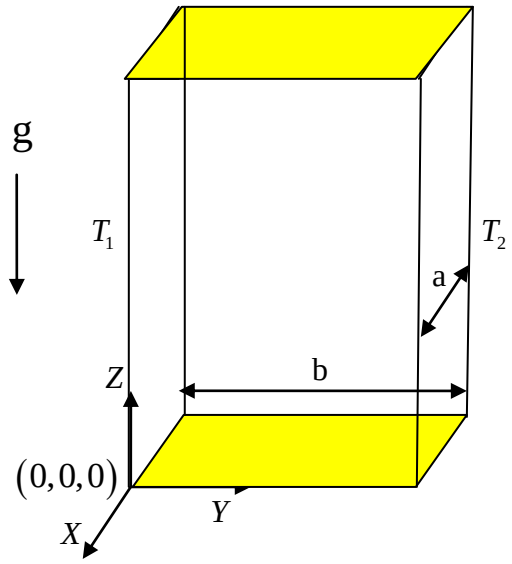

Figure 1. Physical configuration.

The flow is fully developed and the following relations apply here

$$U=V=0,\ \frac{\partial U}{\partial X}=\frac{\partial U}{\partial Y}=\frac{\partial V}{\partial X}=\frac{\partial V}{\partial Y}=0,\ \frac{\partial P}{\partial X}=\frac{\partial P}{\partial Y}=\frac{\partial P}{\partial Z}=0 \tag{1}$$

Therefore, the continuity equation gives $\frac{\partial W}{\partial Z}=0$. One can thus conclude that W does not depend on Z, i.e. $W=W(X,Y)$. Under these assumptions equations governing the flow are

$$\mu\left(\frac{\partial^2 W}{\partial X^2}+\frac{\partial^2 W}{\partial Y^2}\right)+g\rho\beta\left(T-T_0\right)=0 \tag{2}$$

$$\frac{\partial^2 T}{\partial X^2}+\frac{\partial^2 T}{\partial Y^2}+\frac{\mu}{K}\left[\left(\frac{\partial W}{\partial X}\right)^2+\left(\frac{\partial W}{\partial Y}\right)^2\right]=0 \tag{3}$$

Equations (2) and (3) are solved subject to the following boundary conditions:

$$\begin{aligned} &W=0,\quad T=T_1 \quad at\quad Y=0 \quad for\ \ 0\le X\le a\\ &W=0,\quad T=T_2 \quad at\quad Y=b \quad for\ \ 0\le X\le a\\ &W=0,\quad \frac{\partial T}{\partial X}=0 \quad at\quad X=0 \quad for\ \ 0\le Y\le b\\ &W=0,\quad \frac{\partial T}{\partial X}=0 \quad at\quad X=a \quad for\ \ 0\le Y\le b \end{aligned} \tag{4}$$

The above equations can be converted to non-dimensional form using the following non-dimensional parameters

$$x=\frac{X}{b},\ y=\frac{Y}{b},\ w=\frac{W\rho b}{\mu},\ \theta=\frac{T-T_0}{T_2-T_1},\ T_0=\frac{T_1+T_2}{2},$$

$$GR=\frac{g\beta\Delta T\, b^3\rho^2}{\mu^2},\ BR=\frac{\mu^3}{K\Delta T\,\rho^2 b^2} \tag{5}$$

The non-dimensional momentum and energy equations are written as follows.

$$\frac{\partial^2 w}{\partial x^2}+\frac{\partial^2 w}{\partial y^2}+GR\,\theta=0 \tag{6}$$

$$\frac{\partial^2\theta}{\partial x^2}+\frac{\partial^2\theta}{\partial y^2}+BR\left[\left(\frac{\partial w}{\partial x}\right)^2+\left(\frac{\partial w}{\partial y}\right)^2\right]=0 \tag{7}$$

The boundary conditions, used to solve the Eqs. (6) and (7) are as follows.

$$\begin{aligned} &w=0,\ \theta=-\frac{1}{2}\ \ at\ \ y=0\ \ \ for\ 0\le x\le A\\ &w=0,\ \theta=\frac{1}{2}\ \ at\ \ y=1\ \ \ for\ 0\le x\le A\\ &w=0,\ \frac{\partial\theta}{\partial x}=0\ \ at\ \ x=0\ \ and\ \ x=A\ \ \ for\ 0\le y\le 1 \end{aligned} \tag{8}$$

3. METHOD Of SOLUTION

The non-dimensional governing Eqs. (6) and (7) along with the boundary conditions (8) were descretized using Finite Difference Technique. In numerical procedure computational domain is divided into a uniform grid system. Both the second-derivative and the squared first-derivative terms are discretized using the central difference of second-order accuracy. The finite difference form of $\frac{\partial^2 w}{\partial x^2}$ and $\frac{\partial w}{\partial x}$, for example, were discretized as $\frac{\partial^2 w}{\partial x^2}=\frac{w_{i+1,j}-2w_{i,j}+w_{i-1,j}}{\Delta x^2}+O\left(\Delta x^2\right)$ and $\frac{\partial w}{\partial x}=\frac{w_{i+1,j}-w_{i-1,j}}{2\Delta x}+O\left(\Delta x^2\right)$, respectively. Therefore the resultant difference equations are

$$\frac{w_{i+1,j}-2w_{i,j}+w_{i-1,j}}{\Delta x^2}+\frac{w_{i,j+1}-2w_{i,j}+w_{i,j-1}}{\Delta y^2}+GR\,\theta_{i,j}=0 \tag{9}$$

$$\frac{\theta_{i+1,j}-2\theta_{i,j}+\theta_{i-1,j}}{\Delta x^2}+\frac{\theta_{i,j+1}-2\theta_{i,j}+\theta_{i,j-1}}{\Delta y^2}$$
$$+BR\left[\left(\frac{w_{i+1,j}-w_{i-1,j}}{2\Delta x}\right)^2+\left(\frac{w_{i,j+1}-w_{i,j-1}}{2\Delta y}\right)^2\right]=0 \quad (10)$$

and the corresponding discretized boundary conditions are

$$w_{i,0}=-w_{i,1},\ \theta_{i,0}=-1-\theta_{i,1},$$
$$w_{i,Ny+1}=-w_{i,Ny},\ \theta_{i,Ny+1}=1-\theta_{i,Ny},$$
$$w_{0,j}=-w_{1,j},\ \theta_{0,j}=\theta_{1,j},$$
$$w_{Nx+1,j}=-w_{Nx,j},\ \theta_{Nx+1,j}=\theta_{Nx,j} \quad (11)$$

where i and j range from 1 to Nx and 1 to Ny, respectively. Nx and Ny denote the number of grids inside the computational domain in the respective x and y directions. With the given parameters GR, BR and A, the values of $w_{i,j}$ and $\theta_{i,j}$, after setting the boundary conditions (11), are iterated according to the difference equations (9) and (10). Until all the values of $w_{i,j}$ and $\theta_{i,j}$ in the grid system are less than a prescribed tolerance, the solutions are assumed to be sought.

To validate the present numerical method a study of grid-independence is performed. Solutions of the cases in various uniform mesh of grid size 20×20 (20 grids in both the x and y directions), 40×40, 100×100, and 160×160 are obtained. We compute the results of the dimensionless axial velocity w along the centerline y = 0.5. In general, the numerical results on 20×20, 40×40, 100×100 and 160×160 grids are quite similar. The results show that the maximum difference between the solution of w on the 20×20 grids and that on the finest grids 160×160 is about 0.001, whereas the solutions on 100×100 and 160×160 are almost coherent. The computational results of the dimensionless temperature θ along the centerline y = 0.5 also show that the solutions on grids 100×100 and grids 160×160 are quite consistent. From the image of the grid-independence study, we divide the computational domain of present flow into 100 grids in the y-direction and $100\times A$ grids in the x-direction. The solutions are assumed to be obtained when all elements in the grids are less than 10^{-14} after a suitable number of iterations.

4. RESULTS AND DISCUSSION

In the present study a numerical investigation of flow and heat transfer in a vertical rectangular duct is considered. The basic governing coupled nonlinear partial differential equations are solved numerically using finite difference technique. The results are drawn and shown graphically for different values of Grashof number GR, Brinkman number BR and aspect ratio A on the velocity and temperature fields. The shear stress and rate of heat transfer at both the walls is tabulated. In all the graphs, the pictures above the line contours are the three-dimensional pictures which are drawn to view the direction of flow in the upward and downward flow in a vertical rectangular duct. Further to understand in a better way the flow nature, graphs are also drawn fixing the value of y at 0.5 and varying x from 0 to 1 for all the governing parameters.

Figures 2a,b to 4a,b illustrate the velocity and temperature contours for various values of $GR=1-20$, $BR=0-8$ and $A=0.5-2.0$ with insulated top and bottom walls and isothermal heated vertical walls. Fluid raise up from the middle portion of the vertical wall and flow down along two horizontal walls forming symmetric rolls with clockwise and anti-clockwise rotation inside the cavity. The temperature contours are smooth curve which span the entire enclosure and they are generally symmetric with respect to horizontal symmetric line.

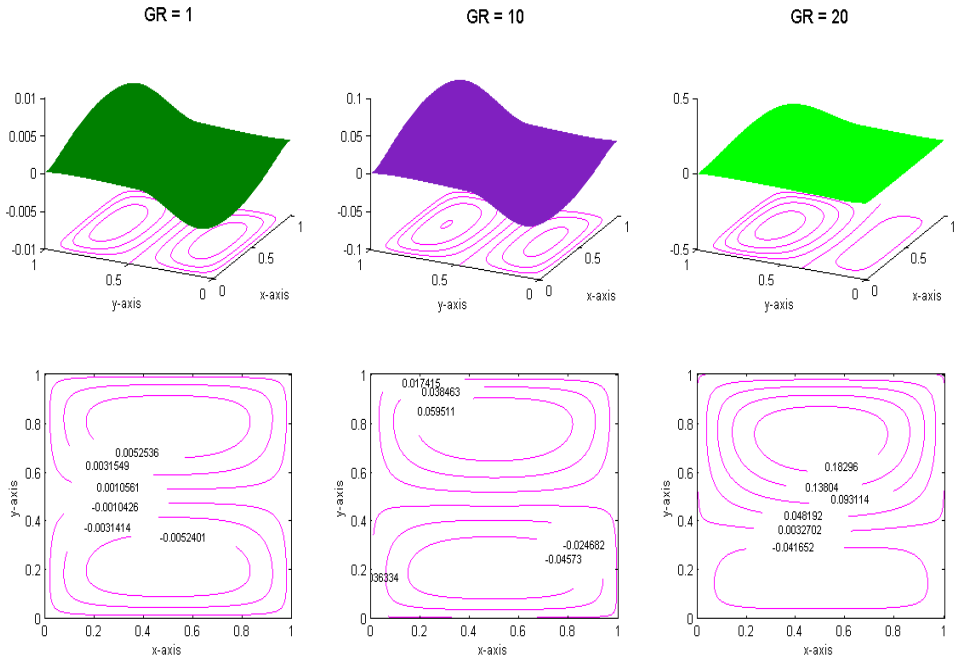

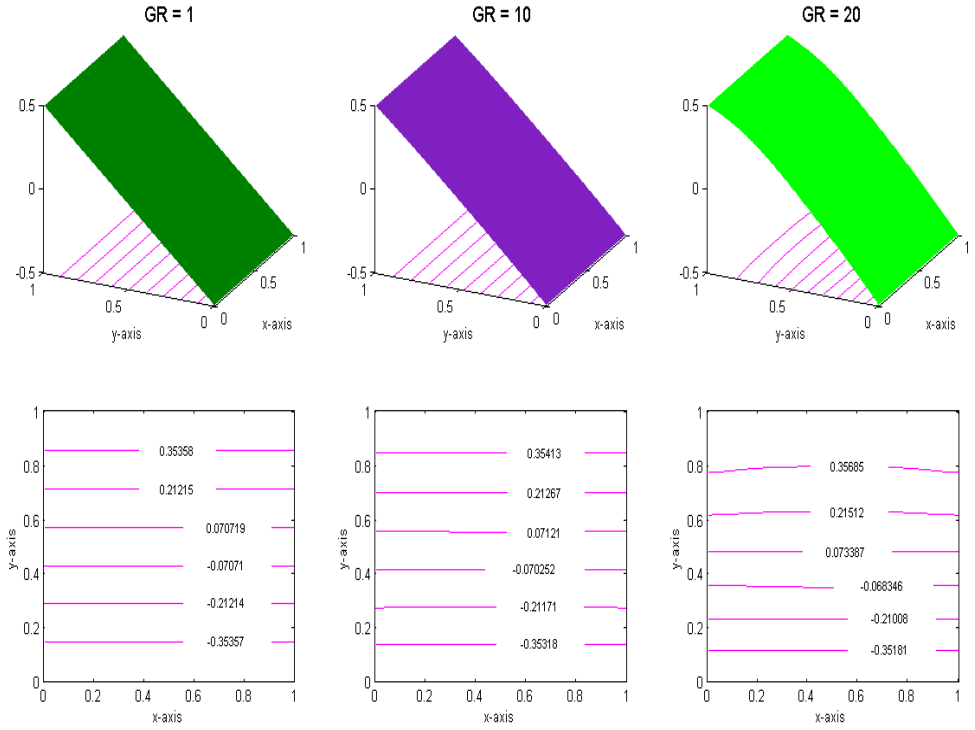

Figure 2a. Velocity and temperature contours for different values of Grashof number GR for BR = 2 and A =1.

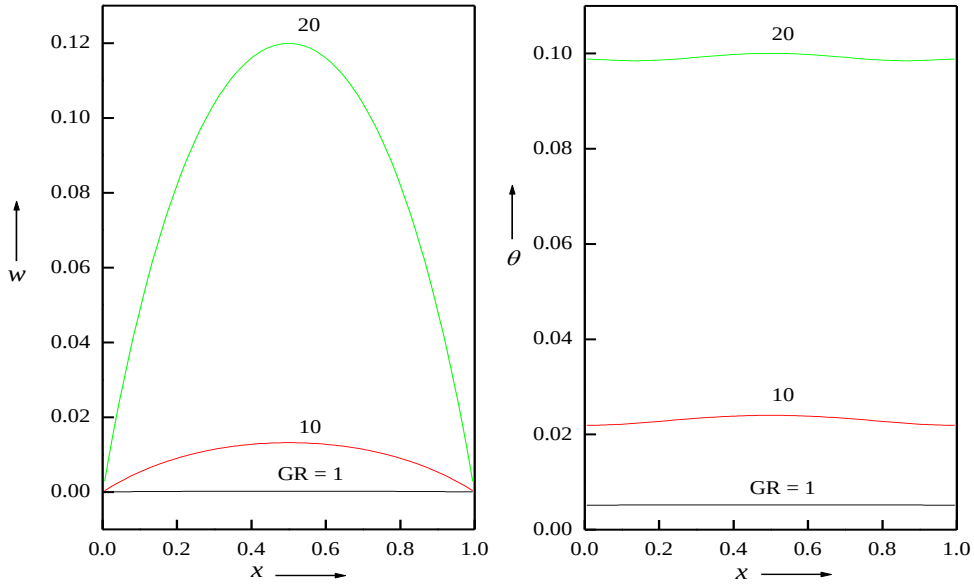

Figure 2b. Velocity and temperature profiles for different values of Grashof number GR for BR = 2 and A =1.

Figure 2a display the effect of Grashof number in a square duct. The Grashof number seems to increase the volume flow rate. That is, as the Grashof number increases, velocity increases in the upward direction and reverses its direction in the downward direction as can be seen in Fig. 2a and that for $GR = 20$, the velocity contour is flat in the downward direction. A nearly symmetric distribution of velocity w above the mid-section can also be observed. The temperature contours become non-linear as the GR increases. It is seen that the temperature contours are nearly linear for small values of GR and the temperature contour with $GR = 20$ starts getting shifted towards the upper wall. The presence of significant convection is also exhibited in Fig. 2a at $GR = 20$ where temperature contour at $y = 0.6$ starts getting deformed and pushed towards the top plate. Further, at $GR = 20$ the circulation is pushed towards the upper part of the cavity and due to enhanced convection from the hot vertical wall, the velocity contours greater than $y = 0.4$ covers almost 70% of the cavity. This is an expected result because physically an increase in the buoyancy force results in support of the motion. It is also seen very clearly from Fig. 2b (one dimension) that as the Grashof number increases both the velocity and temperature

increases significantly and the temperature profiles become non-linear for large values of GR.

The effect of Brinkman number BR on the velocity and temperature contours and profiles is shown in Figs. 3a and 3b respectively. The velocity and temperature contours show similar flow structure as that of Grashof number. That is, as the Brinkman number increases, velocity increases in the upward direction and become flat in the downward direction. The temperature contour show non-linear nature as BR increases. Here also the temperature contours at $y = 0.6$ starts getting deformed and pushed towards the top plate. Figure 3b clearly shows that as BR increases both the velocity and temperature increases fixing $y = 0.5$ for variations of x from 0 to 1. This flow nature is due to the fact that an increase in the Brinkman number results an increase of viscous dissipation effect which results an increase of temperature and as a consequence velocity increases for the increase in buoyancy force in the momentum equation.

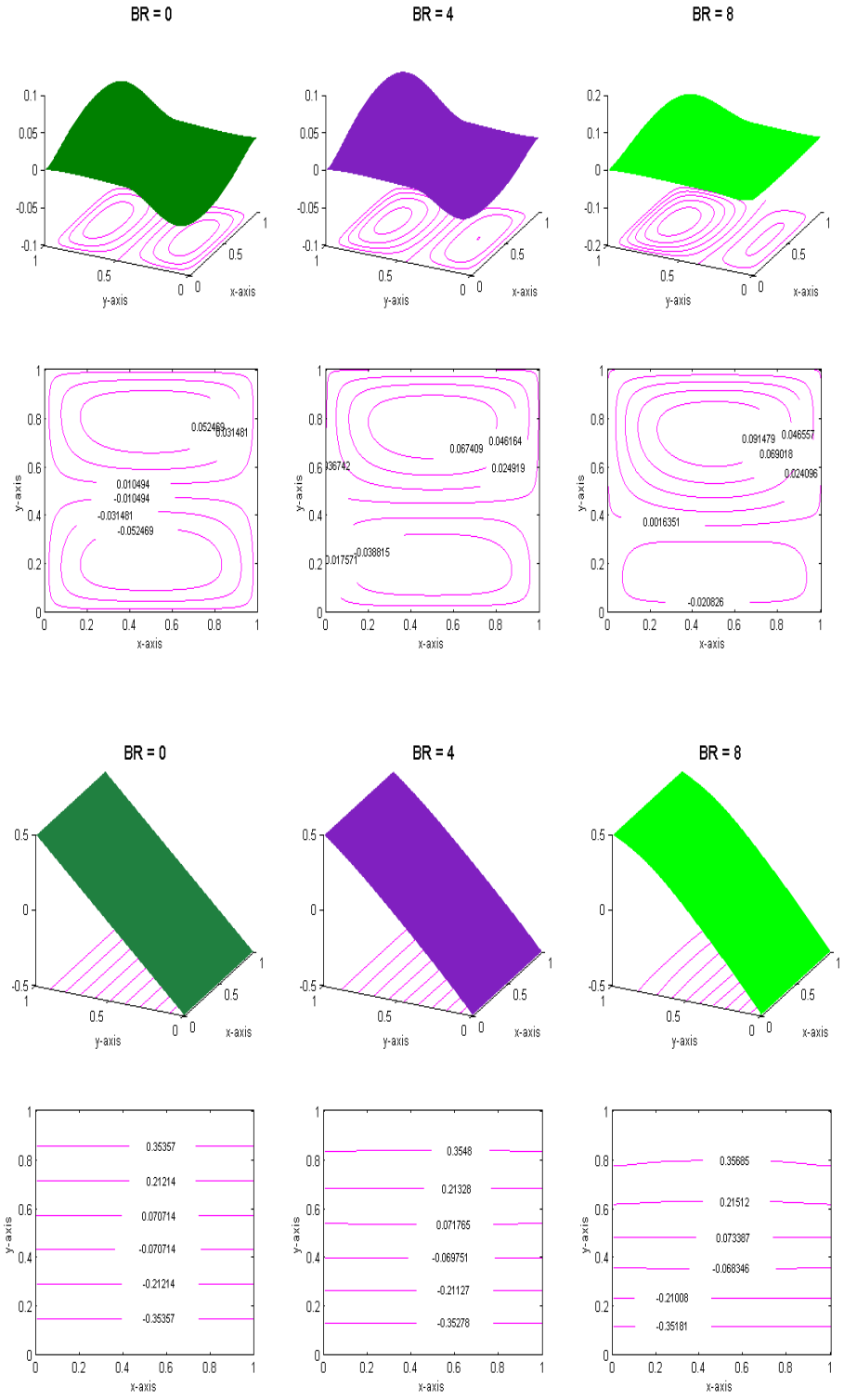

Figure 3a. Velocity and temperature contours for different values of Brinkman number BR for $GR = 10$ and $A = 1$.

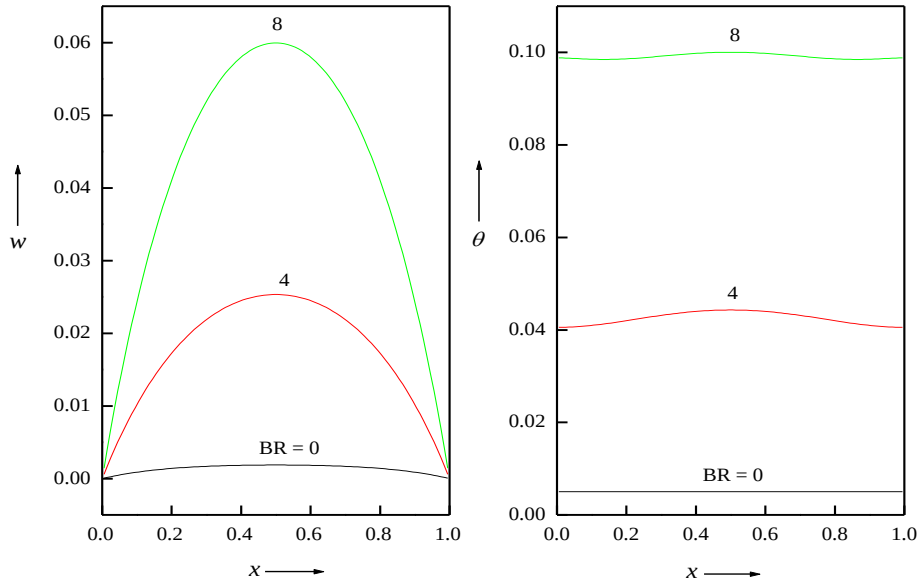

Figure 3b. Velocity and temperature profiles for different values of Brinkman number *BR* for *GR* = 10 and *A* =1.

The effect of aspect ratio A on the velocity and temperature contours is shown in Fig. 4a. As the aspect ratio increases the velocity and temperature contours look more flat for large aspect ratio than that for small aspect ratio. This indicates that for duct of large A, the average velocity or the normalized flow rate should be greater than that for smaller A. It is also seen in Fig. 4a that the velocity and temperature profiles at $y = 0.5$ become flat at the centre as A increases.

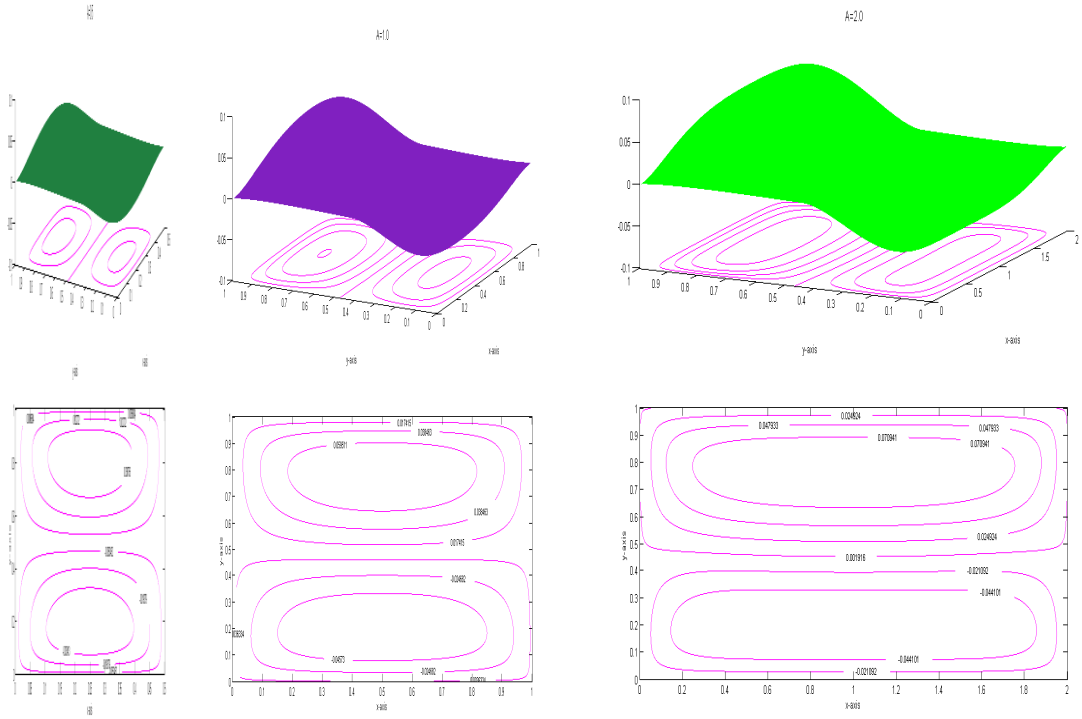

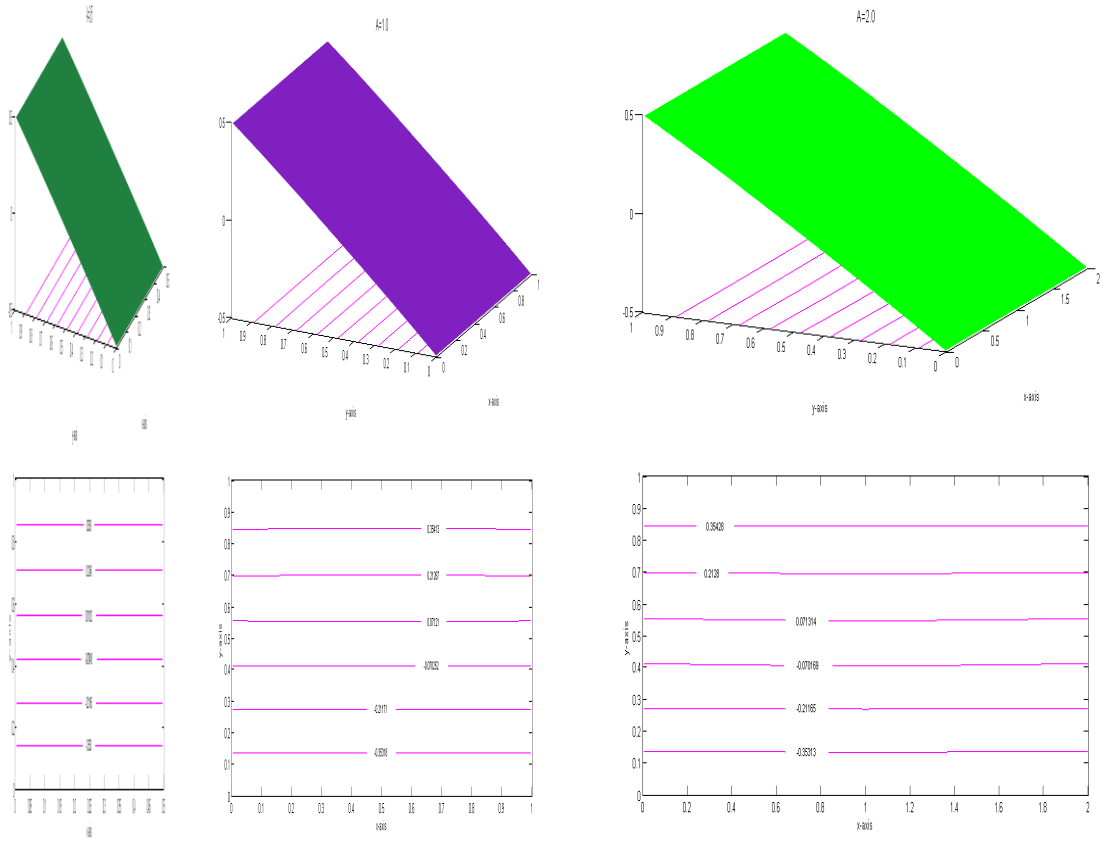

Figure 4a. Velocity and temperature contours for different values of Aspect ratio A for $GR = 20$ and $BR = 2$.

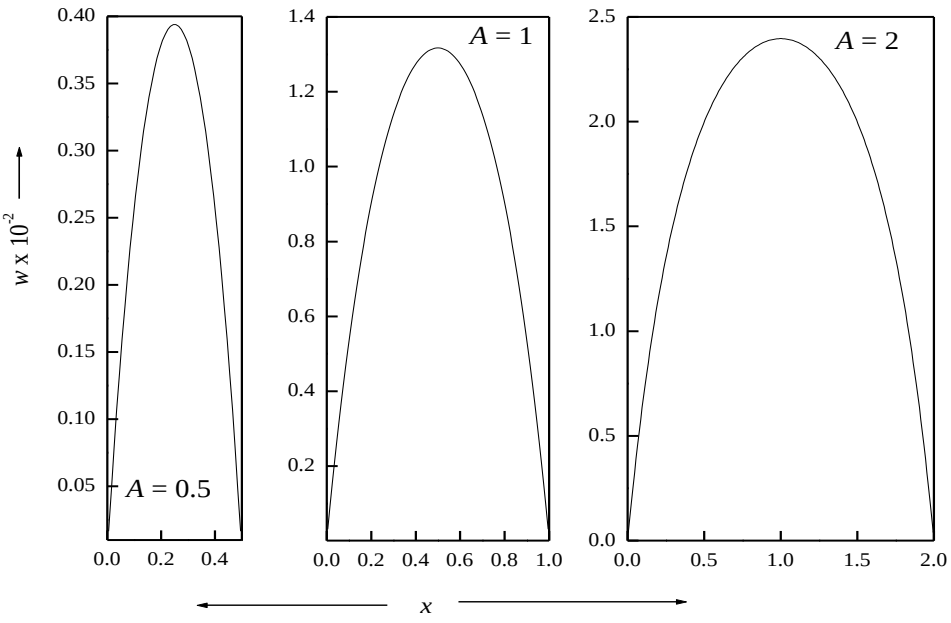

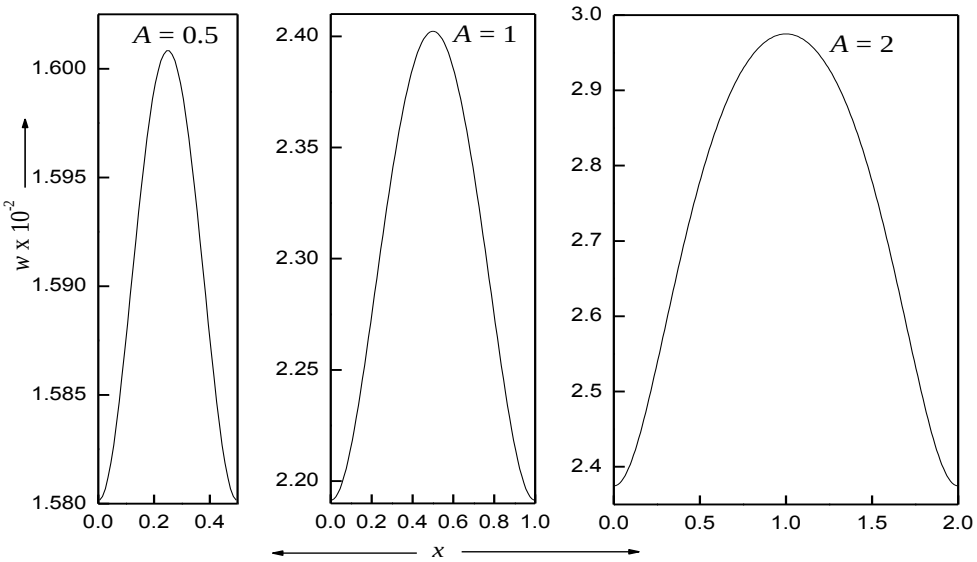

Figure 4b. Velocity and temperature profiles for different values of Aspect ratio A for $GR = 20$ and $BR = 2$.

The volumetric flow rate increases for all the governing parameters such as Grashof number, Brinkman number and aspect ratio as seen in Table-1. The values of shear stress or magnitude of velocity gradient $\frac{\partial w}{\partial y}$ at $y = 0$ and at $y = 1$ increases in magnitude for increasing values of Grashof number and aspect ratio whereas it decreases with Brinkman number. Similar nature is observed for the velocity gradient $\frac{\partial w}{\partial x}$ at $x = 0$ and at $x = 1$ for Grashof number and aspect ratio whereas as Brinkman number increases $\frac{\partial w}{\partial x}$ at $x = 0$ and at $x = 1$ increases. The rate of heat transfer $\frac{\partial \theta}{\partial y}$ at $y = 0$ increases and $\frac{\partial \theta}{\partial y}$ at $y = 1$ decreases for increase in values of Grashof number, Brinkman number and aspect ratio as seen in Table-2.

Table 1: Values of shear stress for different GR, BR and A.

GR	BR	A	q	$\left.\frac{\partial w}{\partial y}\right\|_{y=0}$	$\left.\frac{\partial w}{\partial y}\right\|_{y=1}$	$\left.\frac{\partial w}{\partial x}\right\|_{x=0}$	$\left.\frac{\partial w}{\partial x}\right\|_{x=1}$
1	2.0	1.0	4.923E-6	-3.198E-2	-3.201E-2	1.702E-5	-1.702E-5
10	2.0	1.0	4.982E-3	-0.307491	-0.332994	1.724E-2	-1.724E-2
20	2.0	1.0	5.157E-2	-0.518774	-0.782498	0.180987	-0.180987
10	0.0	1.0	-8.6E-12	-0.319992	-0.319992	-2.6E-11	2.565E-11
10	4.0	1.0	1.035E-2	-0.294543	-0.347531	3.591E-2	-3.591E-2
10	8.0	1.0	2.578E-2	-0.259387	-0.391249	9.049E-2	-9.049E-2
10	2.0	0.5	1.249E-3	-0.232879	-0.239682	7.915E-3	-7.915E-3
10	2.0	1.0	4.982E-3	-0.307491	-0.332994	1.724E-2	-1.724E-2
10	2.0	2.0	1.008E-2	-0.343143	-0.393958	2.155E-2	-2.155E-2

Table 2: Values of rate of heat transfer for different GR, BR and A.

GR	BR	A	$\left.\frac{\partial \theta}{\partial y}\right\|_{y=0}$	$\left.\frac{\partial \theta}{\partial y}\right\|_{y=1}$
1	2.0	1.0	0.500482908161611	0.499516427802567
10	2.0	1.0	0.545424263791710	0.447848031316070
20	2.0	1.0	0.669608471415731	0.187881727677714
10	0.0	1.0	0.499999999974030	0.500000000025496
10	4.0	1.0	0.586597188318810	0.385340066881363
10	8.0	1.0	0.669608471408237	0.187881727702636
10	2.0	0.5	0.529549020658930	0.468434767413300
10	2.0	1.0	0.545424263791710	0.447848031316070
10	2.0	2.0	0.553618753606890	0.433873749412651

5. CONCLUSIONS

The effects of Grashof number, Brinkman number and aspect ratio on the flow and heat transfer of fully developed convective flow in a vertical rectangular duct is analyzed and are shown in pictures and tables. It was found that

1. The velocity and temperature increases with increase in Grashof number, Brinkman number and aspect ratio. The increase in Grashof number and Brinkman number increases the flow in the upward direction and becomes flat in the downward direction. The increase in the aspect ratio results in flattening of the velocity contours.
2. The volumetric flow rate increases with increase in Grashof number, Brinkman number and aspect ratio.
3. The velocity gradient $\frac{\partial w}{\partial y}$ at $y=0$ and at $y=1$ increases in magnitude for increasing values of Grashof number and aspect ratio whereas it decreases with Brinkman number. Similar nature is observed for the velocity gradient $\frac{\partial w}{\partial x}$ at $x=0$ and at $x=1$ for Grashof number and aspect ratio whereas as Brinkman number increases $\frac{\partial w}{\partial x}$ at $x=0$ and at $x=1$ increases.
4. The rate of heat transfer $\frac{\partial \theta}{\partial y}$ at $y=0$ increases and $\frac{\partial \theta}{\partial y}$ at $y=1$ decreases for increase in values of Grashof number, Brinkman number and aspect ratio.

REFERENCES

[1] T. Fusegi, J.M. Hyun, K. Kuwahara, Natural convection in a differentially heated square cavity with internal heat generation. *Numer. Heat Transfer Part A*, vol. 21, pp. 215-229, 1992.

[2] J.L. Lage, A, Bejan, The *Ra-Pr* domain of laminar natural convection in a enclosure heated from the side. *Numer. Heat Transfer Part A*, vol. 19, pp.21-41, 1991.

[3] J.L. Lage, A, Bejan, The resonance of natural convection in a enclosure heated periodically from the side. *Int. J. Heat Mass Transfer*, vol. 36, pp. 2027-2038, 1993.

[4] C. Xia, J.Y. Murthy, Buoyancy-driven flow transitions in deep cavities heated from bellow. *ASME Trans. J. Heat Transfer*, vol. 124, pp. 650-659, 2002.

[5] M. November, W.M. Nansteen, Natural convection in rectangular enclosures from below and cooled along one side. *Int. J. Heat Mass Transfer*, vol. 30, pp. 2433-2440, 1987.

[6] A. Valencia, R.L. Frederick, Heat transfer in a square cavities with partially active vertical walls. *Int. J. Heat Mass Transfer*, vol. 32, pp. 1567-1574, 1989.

[7] M.W. Ganzarolli, L.F. Milanez, Natural convection in a rectangular enclosures heated from bellow and symmetrically cooled from the sides. *Int. J. Heat Mass Transfer*, vol. 38, pp. 1063-1073, 1995.

[8] M. Corcione, Effects of the thermal boundaries conditions at the side-walls upon natural convection in rectangular enclosures heated from below and cooled from above. *Int. J. Heat Mass Transfer*, vol. 42, pp. 199-208, 2003.

[9] B. Gebhart, Y. Jaluriya, R.L. Mahajan, B. Sammkia, Buoyancy-Induced Flows and Heat Transfer. Hemisphere, New York, pp. 737-761, 1998.

[10] A. Bejan, A synthesis of analytical results for natural convection heat transfer across rectangular enclosures. *Int. J. Heat Mass Transfer*, vol. 23, pp. 723-726, 1980.

[11] A.E. Gill, The boundary layer regime for convection in a rectangular cavity. *J. Fluid Mech.*, vol. 26, pp. 515-536, 1966.

[12] A. Bejan, Note on Gill's solution for free convection in a vertical enclosure. *J. Fluid Mech.*, vol. 90, pp. 516-568, 1979.

[13] D.E. Cormack, L.G. Leal, J. Imberger, Natural convection in a shallow cavity with differentially heated end walls – Part I. Asymptotic theory. *J. Fluid Mech.*, vol. 65, pp. 209-229, 1974.

[14] A. Bejan, C.L. Tien, Laminar natural convection heat transfer in a horizontal cavity with different end temperatures. *ASME J. Heat Transfer*, vol. 100, pp. 641-647, 1978.

[15] G.S. Shiralkar, C.L. Tien, A numerical study of laminar natural convection in shallow cavities. *ASME J. Heat Transfer*, vol. 103, pp. 226-231, 1981.

[16] H. Ozoe, H. Sayama, S.W. Churchill, Natural convection in an inclined rectangular channel at various aspect ratios and angles – experimental measurements. *Int. J. Heat Mass Transfer*, vol. 18, pp. 1425-1431, 1975.

[17] G. De Vahl Davis, Natural convection of air in a square cavity: A bench mark numerical solution. *Int. J. Numer. Methods Fluids*, vol. 3, pp. 249-264, 1983.

[18] F.J. Hamadi, J.R. Lloyd, H.Q. Yang, K.T. Yang, Study of local natural convection heat transfer in an inclined enclosure. *Int J Heat Mass Transfer*, vol. 32, pp. 1697-1708, 1989.

[19] L. Adjlout, O. Imine, A. Azzi, M. Belkadi, Laminar natural convection in an inclined cavity with a wavy wall. *Int. J. Heat Mass Transfer*, vol. 45, pp. 2141-2152, 2002.

[20] D. Bercovici, Generation of plate tectonics from lithosphere-mantle flow and void-volatile self-lubrication. *Earth Planetary Sci. Lett.*, vol. 154, pp. 139-151, 1998.

[21] G.P. Celata, G.L. Morini, V. Marconi, S.J. McPhail, G. Zummo, Using viscous heating to determine the friction factor in microchannels – An experimental validation. *Exp. Thermal Fluid Sci.*, vol. 30, pp. 725-731, 2006.

[22] Y. Murakami, B. Mikic, Parametric investigation of viscous dissipation effects on optimized air cooling micro channeled heat sinks. *Heat Transfer Engng.*, vol. 24, pp. 53-62, 2003.

Nomenclature

BR	Brinkman number
GR	Grashof number
g	acceleration due to gravity
K	thermal conductivity of the fluid
$Nx,\ Ny$	grid number in computational domain
T	fluid temperature
T_0	reference temperature
T_1 , T_2	temperatures of the walls of the duct
W	velocity in the Z -direction
X, Y, Z	Cartesian coordinates

Greek letters

β	coefficient of thermal expansion
ρ_0	density of the fluid
ν	kinematic viscosity
μ	viscosity
θ	dimensionless temperature